Four phase hydrate equilibria of methane and carbon dioxide with heavy hydrate former compounds: Experimental measurements and thermodynamic modeling

Hamed Tavasoli and Farzaneh Feyzi[†]

Thermodynamic Research Laboratory, School of Chemical Engineering,
Iran University of Science and Technology, Tehran 16846-13114, Iran

Abstract−We experimentally investigated the hydrate dissociation condition for four phase hydrate (H)-aqueous liquid (L_{Aq})-hydrocarbon rich liquid (L_{HC})-vapor (V) for the ternary systems of help gas-heavy hydrate former-water. Methane and carbon dioxide are known as help gases and benzene and cyclohexane are considered as heavy hydrate formers. The experimental data were generated using an isochoric pressure-search method. Two different equations of state (EOS) were employed to study the equilibrium phase behavior of ternary four phase systems. The EOSs considered are Valderama-Patel-Teja EOS combined with non-density dependent mixing rule (VPT+NDD) and Statistical Associating Fluid Theory EOS proposed by Huang and Radosz (SAFT-HR). The required binary interaction parameters (BIP) were obtained using vapor-liquid equilibrium (VLE) and liquid-liquid equilibrium (LLE) data. The hydrate phase was modeled by the modification of the solid solution theory of van der Waals and Platteeuw. To obtain reliable results, distortion of cages due to occupation of large molecules was considered. The Kihara parameters of cyclohexane were adjusted to hydrate dissociation data. Model calculations for hydrate forming conditions were found to be in satisfactory agreement with the newly reported data in this work and literature data.

Keywords: Gas Hydrate, Four-phase Equilibrium, Heavy Hydrate Formers

INTRODUCTION

Gas hydrates are ice-like compounds which can be formed above the ice point. Gas hydrates consist of water molecules that are hydrogen-bonded to form host cavities with guest molecules inside the cavities. The cavities are able to encapsulate suitably sized guest compounds, which are generally low molecular weight gases and organic substances under the conditions of low temperature and elevated pressure. The interactions between the guest molecules and the host water cavities are weak van der Waals forces. These interactions are responsible for the stability of hydrate structure.

For gas hydrates to remain stable, a considerable fraction of the available cavities have to be occupied by guest molecules. This is the reason why size and type of guest molecules affect the hydrate structure. Depending on the type of the guest molecule, different hydrate structures could be formed. Each structure is composed of water molecules that form certain number of cavities. Currently, three possible structures for gas hydrates are known: structure I (SI), structure II (SII) and structure H (SH). The differences and the properties of these structures are reviewed in-depth by [1].

Hydrates of structures I and II are more common. Depending on the size of the guest molecule, either small or large cavities could be occupied. The ratio of the van der Waals diameter of the guest molecule to the size of cavities specifies the tendency of the guest molecule to fill one or both types of cavities [1]. Small molecules,

such as methane, could fill both small and large cavities of SI. However, methane is only capable of filling the small cavities of SII. Occupying both types of cavities will increase stability of SI compared to SII and will lead to SI hydrate formation. Nitrogen is smaller than methane and could only fill the small cavities, but, because of the greater number of small cavities in SII compared to SI, nitrogen forms SII hydrate. Large molecules, such as iso-butane and propane, can only occupy large cavities of SII and will form SII hydrate. Larger molecules such as n-butane, benzene and cyclohexane, which are referred to as heavy hydrate formers [2-6], do not form hydrates unless they are accompanied with small molecules (help gas) which help them to increase stability of the hydrate structure.

Filling cavities with large guest molecules may cause distortion of cavities. Generally, hydrate formers of structures I and II do not distort hydrate cavities and, as a result, the lattice parameter would not change [1]. However, it has been shown [7] that larger molecules, such as benzene and tetrahydrofuran, stretch the hydrate lattice. Increase in lattice parameter, which is caused by the size of the guest molecule and results in the increase of the unit cell volume, may have a significant impact on hydrate properties [8-10]. In addition, small changes in lattice parameter will cause significant changes in the hydrate formation pressure [11]. It should also be mentioned that lattice parameter is a function of temperature and pressure.

Gas hydrate formation is the subject of many studies. Several research works have been performed considering gas hydrates as unwelcomed phenomena and there are also the topics which have tried to apply gas hydrate properties in different fields of application to favor it [1,12]. To consider gas hydrates as a technological

[†]To whom correspondence should be addressed.
E-mail: feyzi@iust.ac.ir

interest, knowledge of the phase behavior of these systems is of major importance. The phase equilibrium and thermodynamic stability of gas hydrates have been predicted by the theory of van der Waals and Platteeuw [13]. This theory is based on a model in which guest molecules are dissolved in or adsorbed on the host water lattice as ideal solutions. Some assumptions of the older theory of van der Waals and Platteeuw [13] are improved, which have made the theory still applicable in different interesting fields of hydrate formation.

Because of the possibility of hydrate formation in transportation of unprocessed hydrocarbon reservoir fluids [4,6], and application of hydrate formation in separation of close boiling point mixtures [14], or even promotion of hydrate formation by the help of heavy hydrate formers [15,16], the study of their phase behavior is of great interest.

It is suggested that benzene and cyclohexane form SII hydrate in the presence of help gases such as methane, nitrogen and carbon dioxide [17,18]. Hydrate formation point of benzene with methane [3,19] and hydrate formation point of cyclohexane with methane [20-22] and carbon dioxide [23,24] are reported.

In this work, gas hydrate formation conditions of benzene and cyclohexane in the presence of help gases such as methane and carbon dioxide, are studied. Our main goal was to investigate hydrate formation pressure for four phase equilibrium conditions,

hydrate (H)-aqueous liquid (L_{Aq})-hydrocarbon rich liquid (L_{HC})-vapor (V), experimentally and theoretically. We have generated experimental data using an isochoric pressure-search method [25-27]. To demonstrate the reliability of the experimental method, validation tests were performed and the generated data were compared with literature data [2,3,19-24]. The dissociation data for benzene hydrates with carbon dioxide, as the help gas, were produced in this study. In the theoretical part, the modified theory of van der Waals and Platteeuw model was applied to the hydrate phase. Two well-known equations of state (EOS), Valderrama modification of the Patel-Teja EOS [28] combined with non-density dependent mixing rule (VPT+NDD) [29] and Statistical Associating Fluid Theory proposed by Huang and Radosz (SAFT-HR) EOS [30,31] were applied to the vapor and the two liquid phases in equi-

Table 1. Purities and suppliers of the materials used in this work

Chemical component	Supplier	Purity
Methane	Sabalan oxygen	99.995 (vol%)
Carbon dioxide	Sabalan oxygen	99.995 (vol%)
Benzene	Merck	≥99.5% (extra pure grade)
Cyclohexane	Merck	≥99.5% (extra pure grade)

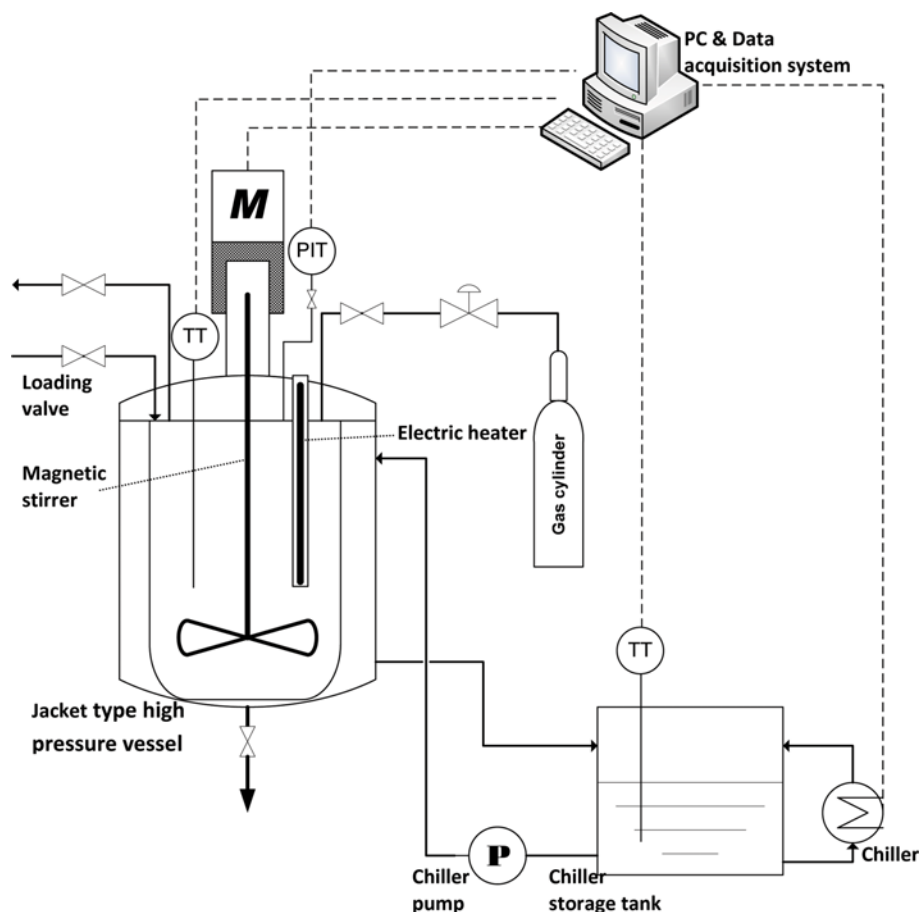Deionized water was used in all the experiments

Fig. 1. Schematic diagram of the experimental apparatus.
　　TT. Temperature transmitter　　　　PIT. Pressure indicator transmitter

librium with the hydrate phase. The required binary interaction parameters (BIPs) for each EOS and also Kihara parameters of cyclohexane were also adjusted.

EXPERIMENTAL SECTION

The main goal of this section is to explain experimental procedure and requirements to investigate hydrate dissociation points for methane+benzene+water, methane+cyclohexane+water, carbon dioxide+cyclohexane+water and carbon dioxide+benzene+ water systems.

1. Chemicals

Table 1 represents the purities and suppliers of the chemicals used in this work.

2. Experimental Apparatus

The main part of the apparatus is a jacketed cylindrical vessel made of 316 stainless steel equipped with side-glass which can withstand pressures up to 15 MPa. The schematic diagram of the apparatus is shown in Fig. 1. The volume of the vessel is approximately 500 cm^3. The vessel is equipped with a magnetic stirrer, which ensures sufficient agitation to facilitate reaching equilibrium. To increase contact between the fluids and enhance conversion of water into hydrate, speed of stirring could be increased up to 1,500 rpm. A platinum resistance thermometer (Pt100) was inserted into the vessel to measure the temperature with the accuracy of ±0.1 K. The pressure in the vessel was measured by a BD pressure transducer (BD, type 30.600G calibrated for pressures up to 10 MPa), calibrated against a dead weight balance. The accuracy of the pressure transducer was ±10 kPa. To control the temperature inside the vessel, mixture of water+ethanol was used as the cooling media against electrical heater as the heating agent. The temperature and the pressure of the vessel and the speed of the magnetic stirrer were recorded every minute.

3. Preparation of the Apparatus

Prior to each run, the vessel was washed and dried. To ensure the absence of any traces of unwanted gas molecules in the vessel, it was evacuated and refilled with the desired gases (help gases) three times. The liquid mixture (250 cm^3 water+50 cm^3 benzene/ cyclohexane) was then added to the cell. The degree of freedom of the system is unity, so the composition of the feed does not affect the results of the experimental tests and only temperature acts as the major independent variable. The help gas (methane/carbon dioxide) was supplied from a high-pressure cylinder through a pressure regulating valve into the vessel. When the temperature and the pressure of the cell are stabilized, temperature controlling program starts.

4. Experimental Procedure

To find the equilibrium conditions of H-L_{Aq}-L_{HC}-V for methane/ carbon dioxide as the help gas and benzene/cyclohexane as the heavy hydrate former, isochoric pressure-search procedure [25-27] was applied in this work. The complete experimental runs consist of two different paths: cooling path, in which the temperature of the cell is decreased stepwise until the hydrate forms, and heating path, in which the temperature of the cell is returned to the initial value. Hydrate formation in the vessel is detected by sudden pressure drop. Both paths intersect each other at the hydrate dissociation point.
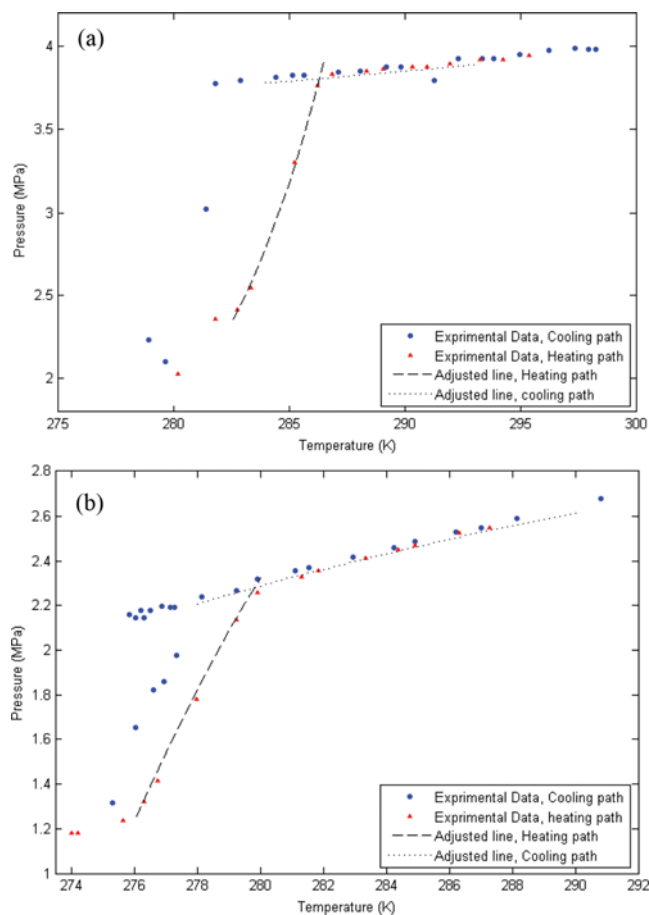
Fig. 2. P−T curves for hydrate formation (a) methane+cyclohexane+ water system and (b) carbon dioxide+cyclohexane+water system. The data are produced in this work. The symbols ● and ▲ denote cooling and heating paths, respectively.

In each of our experimental runs, cooling steps were set at 1 K during 3 hours. To increase accuracy of the heating curve, heating steps were considered such that the thermodynamic equilibrium in each step was achieved. Each step in the heating path was set to 0.5 K. The temperature was kept constant for 6 hours to achieve a steady equilibrium state in the vessel.

As an example of the hydrate formation experiments performed in this work we refer the reader to Fig. 2(a), (b) which presents the hydrate formation conditions for methane+cyclohexane+water and carbon dioxide+cyclohexane+water systems. To find accurate equilibrium hydrate formation point, second-order poly-nominal equations were adjusted to cooling and heating curves and their intersection was found as the hydrate formation point.

Normally, during the cooling path, due to increase of solubility of the gaseous component by lowering the temperature, the pressure is decreased. By further cooling, pressure drops suddenly because of hydrate crystallization. But, for systems in which carbon dioxide is used as one of the hydrate formers, the cooling path does not follow the mentioned common trend of the cooling curve [16]. In such systems, during the cooling path, at the hydrate formation point, a sudden temperature rise could be observed before sudden pressure drop. This rise is caused by the hydrate nucleation

Table 2. Literature review of the experimental data for the dissociation conditions of heavy hydrate formers in the presence of the help gases

Clathrate hydrate system	Hydrate dissociation temperature range/K	Hydrate dissociation pressure range/MPa	References
Methane+benzene	275.45-287.45	1.507-8.57	[3]
	274.2-288.0	1.28-8.98	[19]
Methane+cyclohexane	275.05-290.95	0.779-8.143	[22]
	273.97-291.58	0.684-9.486	[21]
Carbon dioxide+rcyclohexane	274.97-279.8	0.9-2.55	[24]
	275.2-278.1	0.95-1.81	[23]

and growth which is an exothermic phenomenon. The released heat is quickly damped by the temperature controlling system which returns the temperature of the cell to the set point value. The intensity of the temperature peak depends on the nature of the hydrate formation process and the amount of the hydrate former present in the aqueous phase [16].
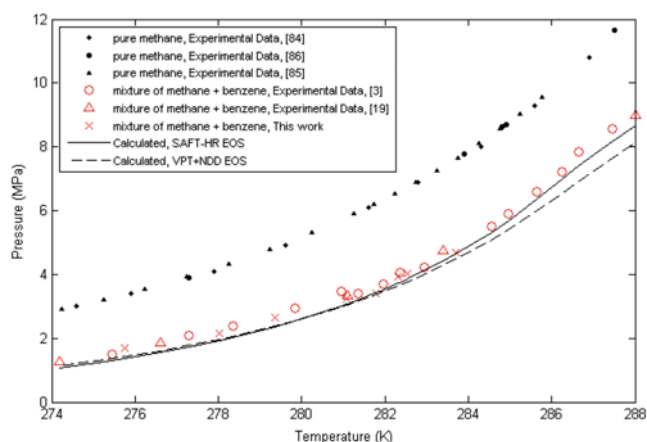
Hydrate formation of methane+benzene/cyclohexane+water and carbon dioxide+cyclohexane+water systems is reported in literature [3,19,21-24]. The corresponding results are summarized in Table 2. To validate our experimental setup and procedure, and

also finding new hydrate dissociation data points, these systems are re-considered in this work. The new results are reported in Table 3 and are compared with literature data in Figs. 3-5. To the

Table 3. Experimental hydrate dissociation data for ternary-four phase (V-H-L_w-L_{Aq}) systems obtained in this work

T/K[*]	Exp. P/MPa[*]
Methane+benzene+water hydrate	
275.7	1.68
278.0	2.17
279.4	2.66
281.1	3.24
281.1	3.25
281.8	3.41
282.3	3.94
282.5	4.02
283.7	4.68
Methane+cyclohexane+water hydrate	
278.4	1.17
280.6	1.76
282.7	2.20
283.8	2.72
285.3	3.42
285.5	3.48
286.4	3.83
287.1	4.46
Carbon dioxide+cyclohexane+water hydrate	
277.7	1.57
278.4	1.83
279.0	2.10
279.7	2.36
Carbon dioxide+benzene+water hydrate	
276.8	1.63
277.4	1.81
278.1	1.99

[*]Standard uncertainties u are u(T)=0.1 K and u(P)=10 kPa

Fig. 3. Experimental and calculated dissociation conditions for clathrate hydrates of methane+water and methane+benzene+water. Symbols represent experimental data. Methane+water hydrate dissociation conditions: ◆: [84], ●: [86], ▲: [85]; methane+benzene+water hydrate dissociation conditions: ✕: This work, ○: [3], △: [19].
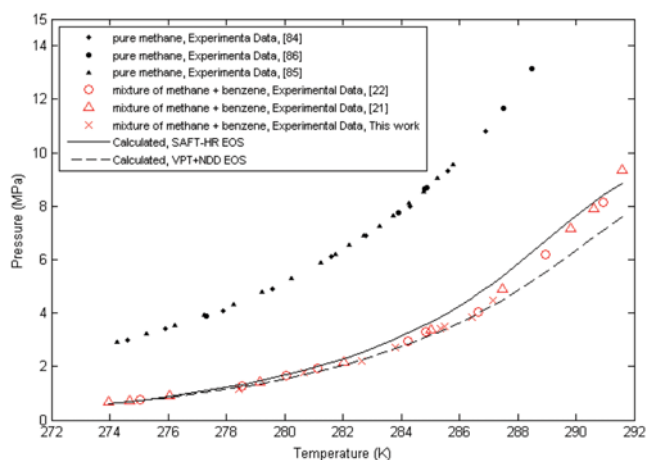
Fig. 4. Experimental and calculated dissociation conditions for clathrate hydrates of methane+water and methane+cyclohexane+water. Symbols represent experimental data. Methane+water hydrate dissociation conditions: ◆: [84], ●: [86], ▲: [85]; methane+cyclohexane+water hydrate dissociation conditions: ✕: This work, ○: [22], △: [21].
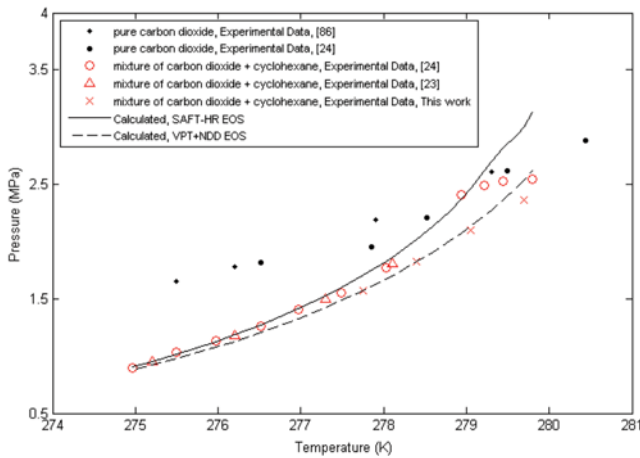
Fig. 5. Experimental and calculated dissociation conditions for clathrate hydrates of carbon dioxide+water and carbon dioxide+cyclohexane+water. Symbols represent experimental data. Carbon dioxide+water hydrate dissociation conditions: ◆: [86], ●: [24]; carbon dioxide+cyclohexane+water hydrate dissociation conditions: ✕: This work, ○: [24], △: [23].
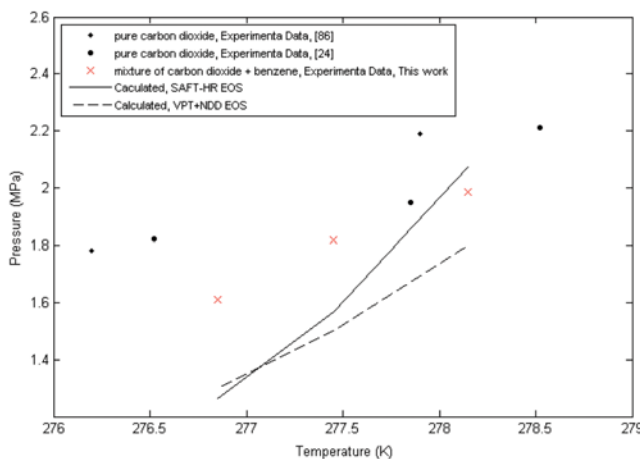

Fig. 6. Experimental and calculated dissociation conditions for clathrate hydrates of carbon dioxide+water and carbon dioxide+benzene+water. Symbols represent experimental data. Carbon dioxide+water hydrate dissociation conditions: ◆: [86], ●: [24]; carbon dioxide+benzene+water hydrate dissociation conditions: ✕: This work.

best of our knowledge hydrate dissociation points for carbon dioxide+benzene+water system, which is obtained in this work, is not reported in literature. The results for this system are reported in Table 3 and Fig. 6.

Based on our experiments the carbon dioxide+benzene+water system needs significantly more nucleation time in comparison with methane+benzene/cyclohexane+water and carbon dioxide+cyclohexane+water systems. To avoid carbon dioxide condensation, initial pressure and temperature for carbon dioxide containing systems should be selected based on upper quintuple point [24].

Due to the nature of four-phase equilibrium systems, reaching to equilibrium conditions is not as easy as three-phase equilibrium systems. For such systems speed of mixing, heating steps and also

the ratio of the amount of heavy hydrate former to water, play significant roles. In four-phase equilibrium systems, more time, high mixing rate and less heavy hydrate former/water ratio are needed to reach the equilibrium conditions. High ratio of heavy hydrate former/water will cause high pressure drop caused by hydrate formation, but due to lower phase contact in such systems, higher mixing rate is needed. In fact, none of these items affect thermodynamic conditions; however, they affect the kinetics of the hydrate formation.

In all the experimental runs in this work, heavy hydrate former/water volumetric ratio, rate of mixing and heating step size were considered to be 1/5, 1,250 rpm and 0.5 K/6 h, respectively.

THERMODYNAMIC FRAMEWORK

The scope of this section is to predict hydrate formation pressure of four phase (H-L_{Aq}-L_{HC}-V) equilibrium conditions. The fugacity-based approach is used. Equality of water fugacity in the co-existing phases is considered as the equilibrium criteria. The fugacity of water in the V, L_{Aq} and L_{HC} phases is calculated by the two well-known VPT+NDD and SAFT-HR EOSs. VPT+NDD EOS is chosen as a cubic EOS which is combined with an elaborate mixing rule and is in common use in hydrate formation calculations, and SAFT-HR EOS is chosen because of the ability of this EOS in modeling mixtures that contain at least one hydrogen bonded component. Our aim has been comparing these EOSs in our calculations.

The fugacity of water in the hydrate phase is calculated by the modified solid solution theory of van der Waals and Platteeuw.

1. Thermodynamic Modeling of Fluid Phases

VPT+NDD EOS, has been extensively used in gas hydrate calculations [3,22,32,33]. The relations and the required parameters can be found in literature [34,35]. In cases where the required BIP was not found in literature, it was either adjusted to liquid-liquid equilibrium (LLE) or vapor-liquid equilibrium (VLE) data. The objective function (OF) used to adjust the BIPs is introduced by Eq. (1).

$$OF = \frac{1}{N}\sum_{i=1}^{N}\left|X_{i,j}^{exp} - X_{i,j}^{cal}\right| \tag{1}$$

In this equation $X_{i,j}^{exp}$ is the experimental solubility and $X_{i,j}^{cal}$ is the calculated solubility of component i in component j, and N denotes the number of data points. The BIPs between water, gaseous and heavy hydrocarbon compounds are presented in Table 4. The references of binary LLE or VLE data which are used for each system are also introduced in Table 4 [36-63].

VPT+NDD EOS [29] favors two types of BIPs, $k_{ij}^{VPT+NDD}$ and l_{ip} which contribute in classical and polar contributions of the mixing rule, respectively. For more explanation we refer the reader to [29]. Both kinds of BIPs are introduced in Table 4.

The second EOS used in this work is the SAFT-HR EOS [30, 31]. All SAFT-HR EOS parameters (three parameters for non-associating compounds and five parameters for associating compounds) are used from literature [30,31], and only the BIPs are adjusted to the aforementioned VLE or LLE data. The BIP term is applied in estimating the dispersion contribution of the SAFT-HR EOS in defining segment energy of binary components [31]. These

Table 4. BIPs for VPT+NDD and SAFT-HR EOSs. A_{ij} and B_{ij} parameters are proposed for calculating the BIPs of SAFT-HR EOS [30,31] according to Eq. (2). l_{ip}^0 and l_{ip}^1 are used in which is suggested by [29]

| Component pair | VPT+NDD EOS | | | Reference | SAFT-HR EOS | | Reference | Sources of VLE and LLE data |
| | l_{ip} | | | | | | | |
	l_{ip}^0	l_{ip}^1			A_{ij}	B_{ij}		
Methane - water	0 .5044[+]	1.8302[+]	51.72[+]	[35]	0.0015	−0.5701	This work	[37,49,54,59,63]
	0.4969[*]	1.8332[*]	58.13[*]					
Carbon dioxide - water	0.19314	0.72280	26.93	[35]	0.0008	−0.3097	This work	[42,58,61]
Benzene - water	0.64327	1.57726	21.00	This work	0.0004	−0.1223	This work	[38,53,55,60]
Cyclohexane - water	0.39788	1.25377	31.4	This work	0.0000	0.0000	This work	[46,51,60]
Methane - benzene	0.05081	0	0	[35]	0.00032	−0.000025	This work	[39,48,50,56]
Carbon dioxide - benzene	0.17565	0	0	[35]	0.00041	−0.04741	This work	[36,44,47]
Methane - cyclohexane	0.01244	0	0	[35]	0.00017	0.03599	This work	[40,57]
Carbon dioxide - cyclohexane	0.18296	0	0	This work	0.00028	0.05047	This work	[36,41,52]
Ethane - water	0.54421	1.5629	32.23	[35]	0.00116	−0.42931	This work	[45,62]
Ethane - cyclohexane	0.01931	0	0	This work	0.00015	−0.02215	This work	[43]

[+]: for 277.13<T≤313.11 K, [*]: for 273.15<T≤277.13 K

BIPs have been considered to be temperature dependent according to the following equation.

$$k_{ij}^{SAFT-HR} = A_{ij} \times T + B_{ij} \qquad T/K \qquad (2)$$

In Eq. (2), T is the temperature. A_{ij} and B_{ij} are adjusted over the entire range of solubility data. The results are presented in Table 4.

2. Thermodynamic Modeling of the Hydrate Phase

Following Klauda and Sandler [64], the fugacity approach model is used to evaluate the hydrate formation conditions. The fugacity of water in the hydrate phase is given by:

$$f_w^{hyd}(T, P) = f_w^\beta(T, P) \exp\left(\frac{-\Delta\mu_w^{hyd}(T, P)}{RT}\right) \qquad (3)$$

where R is the gas constant, f is the fugacity and μ is the chemical potential. Subscript w stands for water and superscript hyd stands for hydrate. The difference between the chemical potential of water in the hypothetical empty (β) and filled (hyd) hydrate is introduced by $\Delta\mu_w^{hyd}(T, P)$.

$$\Delta\mu_w^{hyd} = \mu_w^\beta - \mu_w^{hyd} = -RT\sum_m v_m \ln\left(1 - \sum_j \theta_{mj}\right) \qquad (4)$$

v_m is the number of cavities of type m per water molecule in the lattice and θ_{mj} is defined as the fraction of type m cavities occupied by gas molecules of type j introduced by Eq. (5).

$$\theta_{mj} = \frac{C_{mj}f_j}{\left(1 + \sum_j C_{mj}f_j\right)} \qquad (5)$$

where f_j is the fugacity of component j in the vapor phase (or equally any other coexisting phases in equilibrium) and C_{mj} is the Langmuir constant of component j in cavity of type m that depends on temperature according to Eq. (6). As explained in our previous work [12], multi-layered cavity method introduced by Ballard [65] is a proper method to calculate Langmuir constants. This approach is effective for heavy hydrate formers because non-sphericity of the cavity is considered and the guest molecules fit

better in the certain orientations within the cavity. With this regard, C_{mj} can be calculated from the following equation.

$$C_{mj} = \frac{4\pi}{kT} \int_0^{Rs_1-\alpha_j} \exp\left[\frac{-\sum_n \omega_{jn}(r)}{kT}\right] r^2 dr \qquad (6)$$

In Eq. (6), k is the Boltzmann constant and r is the distance of any point inside the cavity from the center of cavity. The potential function between component j and a given layer n is given by $\omega_{jn}(r)$, where the total potential is given by the sum over all layers. To avoid mathematical singularities, the potential is integrated with spherical symmetry from the center of the cavity to a small distance a_i away from the smallest shell radius (Rs_1).

The interaction potential between guest j and layer n is given by the spherically symmetric Kihara potential function introduced by Eq. (7a) and (7b) [65].

$$\omega_{jn}(r) = 2\varepsilon_j z_n \left[\frac{\sigma_j^{12}}{Rs_n^{11} r}\left(\delta_{jn}^{10} + \frac{\alpha_i}{Rs_n}\delta_{jn}^{11}\right) - \frac{\sigma_j^6}{Rs_n^5 r}\left(\delta_{jn}^4 + \frac{\alpha_j}{Rs_n}\delta_{jn}^5\right) \right] \qquad (7a)$$

$$\delta_{jn}^N = \frac{1}{N}\left[\left(1 - \frac{r}{Rs_n} - \frac{\alpha_j}{Rs_n}\right)^{-N} - \left(1 + \frac{r}{Rs_n} - \frac{\alpha_j}{Rs_n}\right)^{-N}\right], \ N=4, 5, 10, 11 \quad (7b)$$

z_n and Rs_n are the coordination number and the radius of layer of type n, and α_j, ε_j and σ_j are, respectively, the hard core radius, the depth of the intermolecular potential well, and the soft core radius of the encaged guest molecule j. The values of layer coordination number and radius at reference conditions are given in Table 5.

As explained earlier, the nature of the heavy hydrate former component will cause distortion of cavities. To consider the effects of distortion of cavities on Langmuir constants, modifications should be considered. In fact, temperature, pressure and nature of the guest component affect the size of the formed cavity [66-69].

Increasing the temperature and van der Waals diameter of the guest component results in an increase of volume of hydrate cavity, and increasing the pressure leads to a reduction in volume of hydrate cavity. Ballard [65] studied changes of the volume of hy-

Table 5. Cavity parameters in Multi-Layered cage method for structures I and II [65]. These values are measured at reference conditions (T_0=298.15 K and P_0=1 bar)

SI	Small cage (5^{12})		Large cage ($5^{12}6^2$)			
Coordination No. (z)	20		24			
Average radius/Å	3.908		4.326			
Layer type	(i)	(k)	(i)	(k_1)	(k_2)	(c)
Layer coordination No. (z_n)	8	12	8	8	4	4
Layer radius (Rs_{n0})/Å	3.83	3.96	4.47	4.06	4.645	4.25
SII	Small cage (5^{12})		Large cage ($5^{12}6^4$)			
Coordination No. (z)	20		28			
Average radius/Å	3.902		4.683			
Layer type	(a)	(e)	(g)	(e)	(g_1)	(g_2)
Layer coordination No. (z_n)	2	6	12	4	12	12
Layer radius (Rs_{n0})/Å	3.748	3.845	3.956	4.729	4.715	4.635

drate cavities. In summary, their model consists of three separate terms considering effects of temperature, pressure and guest component, separately.

The following expression based on lattice parameter (cubic root of molar volume) is proposed [65] to evaluate changes of hydrate molar volume caused by distortion of cavities.

$$a_H(T, R, \vec{x}) = a_0 \exp\left[\frac{\lambda_1}{3}(T - T_0) + \frac{\lambda_2}{3}(T - T_0)^2 + \frac{\lambda_3}{3}(T - T_0)^3 - \kappa_H(P - P_0)\right] \tag{8}$$

where a_0 denotes the lattice parameter changes due to cavity occupancy at reference conditions T_0 and P_0. Parameters λ_1, λ_2, and λ_3 are thermal expansivity constants of hydrate structure which describe changes of hydrate volume with temperature. And, κ_H is the compressibility constant for each hydrate structure for a certain guest molecule. Repulsive nature of each encapsulated guest molecule

corrects standard lattice parameter values (a_0^*) at T_0, P_0, and the reference composition (x_0). The standard lattice parameters (a_0^*) for SI and SII hydrates are proposed to be chosen as 11.99245 Å and 17.10000 Å, respectively [65]. A detailed discussion and also the complete form of equations can be found elsewhere [1,65,70]. The parameters used in this work are given in Table 6(a), (b), (c). The repulsive nature of guest molecules in each cavity is presented by the repulsive constant, which is introduced in Table 6(c).

The compressibility parameter (κ_H), and the hydrate lattice parameter (a_0) depend on the hydrate structure and composition of the guest(s) molecule in the hydrate lattice, while the thermal expansion coefficients (λ_i), depend only on the hydrate structure.

Based on lattice expansion/compression with temperature, pressure and guest component, the cavities are expanded or compressed. Changes in radius of each cavity will affect the calculated Langmuir constant values. In this regard, it has been proposed [65] that the radius of the layers in each cavity to be a linear function of the

Table 6. (a) Thermal expansivity coefficients for each hydrate structure [65]

	λ_1/K^{-1}	λ_2/K^{-2}	λ_3/K^{-3}
Structure I	3.384960e-4	5.400990e-7	−4.769460e-11
Structure II	2.029776e-4	1.851168e-7	−1.879455e-10

Table 6. (b) Compressibility parameter for each hydrate guest molecule in structures I and II [65]

Component	κ_{SI}/bar^{-1}	κ_{SII}/bar^{-1}
Methane	1.0e-05	5.0e-05
Carbon dioxide	1.0e-06	1.0e-05
Ethane	1.0e-08	1.0e-07
Benzene	0.0	1.0e-08
Cyclohexane	0.0	1.0e-08

Table 6. (c) Repulsive constant for each hydrate guest molecule in each cage of structures I and II [65]

Component	Small cages-SI	Large cages-SI	Small cages-SII	Large cages-SII
Methane	1.7668e-2	0	2.0998e-3	1.1383e-2
Carbon dioxide	0	5.8282e-3	2.2758e-3	1.2242e-2
Ethane	0	2.5154e-2	2.5097e-3	1.4973e-2
Benzene	0	0	0	3.5229e-2
Cyclohexane	0	0	0	3.28e-2

hydrate lattice parameter, as defined by Eq. (9).

$$Rs_n = Rs_{n0} \frac{a}{a_0^*} \qquad (9)$$

where a is the lattice parameter at T, P and x, and Rs_{n0} is the layer radius at referenced conditions. The values of Rs_{n0} are given in Table 5. New values of the layer radius can be updated and applied in calculating the new values of Langmuir constants by trial and error procedure.

Molar volumes of the standard hydrates of SI and SII at T_0 and P_0, are assumed to be the molar volumes of methane (22.7712 cm³/mol) and propane (22.9456 cm³/mol) hydrates, respectively [65]. The guest occupying dependency is removed for the standard empty hydrates and only the effects of temperature and pressure are considered in changes of molar volume of the standard hydrates.

Since all hydrates of a given structure have the same thermal expansion, the values of thermal expansion parameters are equal to their standard empty hydrates. Pressure dependency of molar volume in a filled hydrate is a function of guest occupancy in large cavities. Consequently, to consider the effect of pressure on volume changes of empty hydrate, a different approach should be applied. In calculating the molar volume of empty hydrate the functions should be free of guest dependency. Because of that, a new correction function is proposed in this work to be applied in updating molar volume of empty hydrate due to changes in pressure. The new function depends only on hydrate structure and is introduced as:

$$K_H = \frac{\chi_1}{1 + \exp(\chi_2 - \chi_3(P - P_0))} \qquad (10)$$

In this equation χ_1, χ_2 and χ_3 are structure-dependent parameters and P_0 and P are in bar. The parameters in Eq. (10) are obtained as $\chi_1 = 0.927407$, $\chi_2 = -7.15685$ and $\chi_3 = 0.068739$ for SII hydrate. These values are fitted based on hydrate dissociation condition of methane +benzene+water system. Empty hydrate volume changes can be neglected at low pressures but is significant as the pressure is rised.

$f_w^\beta(T, P)$ in Eq. (3) is the fugacity of the hypothetical empty hydrate lattice at the desired temperature and pressure and is calculated by Eq. (11).

$$f_w^\beta(T, P) = P_w^{sat, \beta}(T) \times \varphi_w^{sat, \beta}(T) \times \exp\left[\frac{v_w^\beta(T, P)(P - P_w^{sat, \beta}(T))}{RT}\right] \qquad (11)$$

In this equation, ν is the molar volume and φ is the fugacity coefficient. Superscript sat refers to saturation. Since the vapor pressure of water is low, fugacity coefficient of water in the empty hydrate lattice ($\varphi_w^{sat, \beta}$), is assumed to be unity. Sloan et al. [71] have suggested the following equations to estimate the vapor pressure of empty hydrate lattice ($P_w^{sat, \beta}$) for structures I and II:

Structure I:

$$P_w^{sat, \beta}/atm = \exp\left(17.44 - \frac{6003.9}{T/K}\right) \qquad (12a)$$

Structure II:

$$P_w^{sat, \beta}/atm = \exp\left(17.332 - \frac{6017.6}{T/K}\right) \qquad (12b)$$

Molar volume of water in the empty lattice (v_w^β), is estimated using the following expression.

$$v_w^\beta(T, P) = v_0^\beta(T_0, P_0) \times \exp[\lambda_1(T - T_0) + \lambda_2(T - T_0)^2 + \lambda_3(T - T_0)^3] \times K_H \qquad (13)$$

In this equation $v_0^\beta(T_0, P_0)$ expresses molar volume of the standard hydrate.

KIHARA PARAMETERS

The Kihara potential model introduced by Eq. (7a) and (7b) contains parameters describing the cavity wall and parameters describing the guest component. The parameters representing the properties of water molecules in the cavity wall, i.e., z_n and Rs_n, are based on the formed hydrate structure (see Table 5), and parameters describing the guest component, i.e., ε, σ and α are commonly based on adjusting on the second virial coefficient and gas viscosity data of a pure substance. The Kihara parameters may also be correlated to hydrate formation data. Unfortunately, the two methods give significantly different values.

To obtain Kihara parameters, based on hydrate formation data, several methods and considerations are proposed to generate reliable and applicable results. Reviews of these methods are given in the literature [65,72-80].

In spite of applying the same adjustment procedure for Kihara parameters based on hydrate dissociation data, there is hardly agreement on the published values [1,73,78,81]. The main reason may be attributed to applying different sources of experimental hydrate dissociation data, considering different values of reference properties of empty hydrate, using different EOS models in modeling fluid phases [76], and finally, the differences in cavity shell consideration.

In this work, for nearly all the compounds considered, the Kihara parameters were obtained from literature [1,65]. Because no Kihara parameters are proposed for cyclohexane by Ballard [65], the parameters should be adjusted by a method similar to Ballard [65]. Different Kihara parameters for cyclohexane are reported in literature [22,42,79,82]. A help gas is needed to form stabilized hydrate structure for cyclohexane, which in this case is SII [83]. Hard core parameter of cyclohexane, obtained from viscosity data, is assumed to be equal to 0.951 Å [79]. Because of a lack of non-dissociation pressure data, in adjusting the parameters of cyclohexane, different dissociation pressure data with different help gases [15,22,24] are used to obtain unique values for ε and σ. Methane, carbon dioxide and ethane are considered as help gases for cyclohexane hydrate formation. The Kihara parameters are independent of temperature [76], but to remove any unexpected effect of temperature on calculation, the temperatures for three different systems are kept nearly equal. The temperature and the related dissociation pressure of the systems used in adjusting the Kihara parameters of cyclohexane are gathered in Table 7.

The difference between fugacities of water in the hydrate and vapor phases is considered as the OF.

$$OF = \left| f_w^{hyd} - f_w^{vap} \right| < 10^{-9} \qquad (14)$$

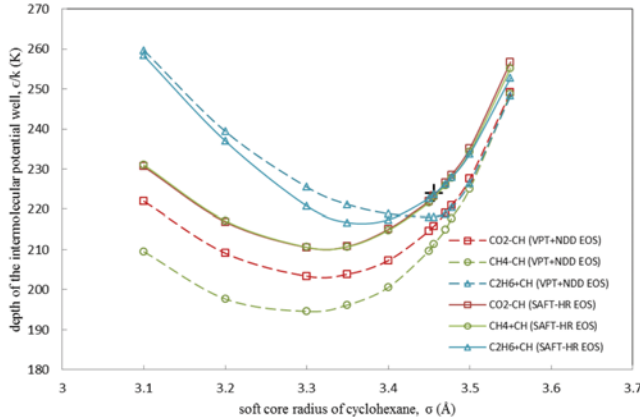To calculate the fugacity of water in the vapor phase, SAFT-HR and VPT+NDD EOSs are applied.

Fig. 7 shows the variation of ε/k as a function of σ. As observed

Table 7. The temperature and related dissociation pressure of the systems used for adjusting the Kihara parameters of cyclohexane

System	T/K	P/MPa	Reference
Methane+cyclohexane+water	275.05	0.779	[22]
Carbon dioxide+cyclohexane+water	274.97	0.900	[24]
Ethane+cyclohexane+water	275.1	0.536	[15]

Fig. 7. Determination of Kihara potential parameters of cyclohexane (CH). Solid lines and dashed lines show adjusted binary values of σ and ε/k obtained by SAFT-HR EOS and VPT+NDD EOS, respectively. The unique values of σ and ε/k is shown by +.

in this figure, for each EOS, three different curves are obtained for each hydrate forming system. To find the optimum unique values for ε and σ, the intersection of the obtained curves is desired.

The applied Kihara parameters for guest components introduced by Ballard [65] or obtained in this work (only for cyclohexane) are shown in Table 8.

Table 8. Kihara parameters for some substances

	α/Å	σ/Å	εk^{-1}/K	Reference
Methane	0.3834	3.14393	155.593	[1,65]
Ethane	0.5651	3.24693	188.181	[1,65]
Carbon dioxide	0.6805	2.97638	175.405	[1,65]
Benzene	1.2	3.25176	223.802	[1,65]
Cyclohexane	0.951	3.456	224.0	This work

Based on Ballard's multi layered approach [65], the same as the adjusted Kihara parameters based on second virial coefficient and viscosity data, the trend of the Kihara parameters versus hard core radius should be linear. It is also claimed that the best suitable value for σ is not located at the minimum of the curve of ε versus σ, but at some distance from this point [77,79]. Based on the obtained values of Kihara parameters for cyclohexane, we conclude that the proposed values are consistent with the two mentioned criteria.

RESULTS AND DISCUSSION

As explained in the experimental section, isochoric pressure search method was used to determine the hydrate dissociation (temperature and pressure) conditions for the systems of methane+benzene/cyclohexane+water and carbon dioxide+benzene/cyclohexane+water. All the experimental data obtained in this work are reported in Table 3 and plotted in Figs. 3-6.

First, hydrate dissociation conditions for the methane+benzene/cyclohexane+water and carbon dioxide+cyclohexane+water systems, for which experimental data are available in literature [3,19-24,79], were measured experimentally. Then, hydrate formation conditions for carbon dioxide+benzene+water were investigated. To the best of our knowledge, no experimental data is available for this system. For each of the mentioned systems four phase (V-H-L_w-L_{Aq}) equilibrium is studied in the thermodynamic modeling part. Degree of freedom of four-phase equilibrium in a ternary

Table 9. Average absolute relative percent deviation (AAD%)* of calculated dissociation pressure for ternary-four phase (V-H-L_w-L_{Aq}) equilibria. The data points used are from [3,19,21-24] and this work

Ternary-four phase system	Source of data	Number of data point (N)	AAD% obtained by applying SAFT-HR EOS	AAD% obtained by applying VPT+NDD EOS
Methane+benzene +water hydrate	This work	9	7.02	7.41
	Literature	19	8.57	10.5
	Total	28	8.09	9.37
Methane+cyclohexane +water hydrate	This work	8	12.83	3.69
	Literature	18	5.56	8.33
	Total	26	8.42	6.95
Carbon dioxide+cyclohexane +water hydrate	This work	4	15.78	2.45
	Literature	15	3.62	5.66
	Total	19	6.18	3.99
Carbon dioxide+benzene +water hydrate	This work	3	13.25	15.35
	Literature			
	Total	3	13.25	15.35

*$AAD\% = \frac{1}{N}\sum\left(\left|P^{exp} - P^{cal}\right|/P^{exp}\right) \times 100$

system is one. Consequently, the initial composition of compounds does not affect the dissociation pressure of hydrate formation at a certain temperature.

The predicted hydrate formation points by the VPT+NDD and SAFT-HR EOS models are also presented in Figs. 3-6. As mentioned, the BIPs are adjusted to VLE or LLE data. The average absolute relative percent deviation (AAD%) of predicted results are introduced in Table 9.

1. Methane+Benzene+Water System

Methane is known to form SI hydrate; however, the hydrate formed in the presence of benzene is SII. The obtained experimental results and the calculated values of dissociation pressure by VPT+NDD and SAFT-HR EOSs for this system are presented in Fig. 3. Hydrate formation of methane+benzene+water system has been investigated by Danesh et al. [3] and Mohammadi et al. [19]. Their results are also demonstrated in Fig. 3. As can be seen, the experimental data obtained in this work are in good agreement with the experimental data reported in literature [3,19].

As is evident in this figure, both EOSs have calculated the experimental points with acceptable accuracy, and the results of calculated hydrate formation conditions over the entire range of temperature are nearly the same for both EOSs. The performance of VPT+NDD EOS in lower pressures is better than at high pressures, while SAFT-HR EOS has shown better results at higher pressure region. In Table 9, the AAD% for the calculated dissociation pressure is presented. AAD% of the data obtained in this work and the data reported in literature [3,19] is given separately. AAD% over the entire range of data is also presented which are 8.09 and 9.37 by SAFT-HR EOS and VPT+NDD EOS, respectively.

2. Methane+Cyclohexane+Water System

Cyclohexane forms SII hydrate in the presence of help gases. The experimental and also calculated hydrate equilibrium conditions are demonstrated in Fig. 4. This system has also been investigated by Sun et al. [21] and Tohidi et al. [22]. As can be observed in Fig. 4, the experimental data obtained in this work are in very good agreement with literature data [21,22]. The calculated hydrate formation condition by VPT+NDD and SAFT-HR EOSs shows the superiority of SAFT-HR EOS, especially at higher pressures.

The AAD% values obtained by use of each EOS are introduced in Table 9. The AAD% for SAFT-HR and VPT+NDD EOSs are reported as 8.42 and 6.95, respectively, over the entire range of experimental data. Predicted results and also estimated AAD% show accuracy of the models and also reliability of the obtained Kihara parameters of cyclohexane.

3. Carbon Dioxide+Cyclohexane+Water System

The phase behavior of carbon dioxide+cyclohexane+water system is more complex. This complexity results from the occurrence of liquid carbon dioxide phase. The upper end point of the four phase equilibrium line (V-L_{Aq}-L_{Hc}-H) is limited to quintuple point at 280.03 K and 2.65 MPa [24]. Because of that, the range of investigation is limited to the lower and upper quintuple points. Hydrate formation points of carbon dioxide+cyclohexane+water system were studied by Mohammadi and Richon [23] and Mooijer-van den Heuvel et al. [24]. The experimental data obtained in this work and the literature data [23,24] are shown in Fig. 5. The obtained data in this work shows acceptable compatibility with literature data in

low temperatures (lower than 279 K) while at higher temperatures our data shows deviation from the data produced by Mooijer-van den Heuvel et al. [24].

SAFT-HR and VPT+NDD EOSs are used to calculate the hydrate formation points. The overall AAD% and also AAD% over experimental data obtained in this work and experimental data reported in literature [23,24] are presented in Table 9. The performance of the EOSs close to the quintuple point is not as good as in low temperature region. The total AAD% obtained by SAFT-HR EOS is 6.18 and by VPT+NDD EOS is 3.99.

4. Carbon Dioxide+Benzene+Water System

Because of the nature of carbon dioxide in the system of carbon dioxide+benzene+water, the four-phase equilibrium line (V-L_{Aq}-L_{Hc}-H) is limited to upper and lower quintuple points. Experimental determination of this point is not in the scope of this work. In this regard, the searching area should be limited to two upper and lower quintuple points. The lower temperature limit is set to 273.15 K and the upper range is estimated by BUBL P calculation. In comparison with former systems, in order to measure the pressure drop of the system, a significant induction time was needed. Several hydrate formation runs were handled and only three reliable equilibrium points were measured for this system. The experimental and calculated results are presented in Fig. 6.

SAFT-HR EOS and VPT+NDD EOSs are both used to obtain the hydrate formation points. The total AAD% is 13.25 and 15.35 for SAFT-HR EOS and VPT+NDD EOS, respectively.

5. Comparison of the Performance of EOS Models

Because of the powerful theoretical background of SAFT-HR EOS [30,31], especially whenever associating molecules such as water are present, it is expected that phase equilibrium calculations lead to more accurate results by this EOS. VPT [28] is a simple cubic EOS, which may not be used in complicated phase equilibrium calculations [29], but the weak points of VPT EOS might be removed by applying more elaborate mixing rules as is proposed by Avlonitis et al. [29]. Application of these mixing rules results in increase of the number of fitting parameters. In VPT+NDD EOS [29] fitting parameters are assigned to asymmetric interactions between polar components and non-polar components. Increasing the number of fitting parameters in VPT+NDD EOS compensates its weak theoretical background and enables this EOS to compete with SAFT-HR EOS.

Comparing the results of modeling we may conclude that both EOS models have produced nearly the same results; however, generally SAFT-HR EOS has performed better at higher pressures. SAFT-HR EOS with its more powerful theoretical background, and VPT+NDD EOS with the help of the mixing rule and more number of adjusted BIPs, are both reliable in these calculations.

The discrepancy between experimental data and the calculated results by sophisticated EOS models arises from a number of factors. Besides the errors of the EOS models, we may refer to the assumptions of the ideal solution theory of van der Waals and Platteeuw model and the values of Kihara parameters.

6. Effect of Addition of Heavy Hydrate Formers on Hydrate Formation Conditions

Figs. 3 and 4 show some selected experimental hydrate dissociation data from literature for methane+water system [84-86] to identify the effect of addition of heavy hydrate formers. Also, in order

to investigate the effect of adding heavy hydrate formers into three phase (V-H-L$_w$) system of carbon dioxide+water, the selected experimental hydrate dissociation data of this system [24,86] is also considered in Figs. 5 and 6.

As can be seen, hydrate formation points are changed significantly to lower pressures and higher temperatures, which is an indication of inclusion of the heavy hydrate formers into hydrate structure. In comparison to benzene, cyclohexane affects methane+water system more significantly.

Generally, adding heavy hydrate formers into methane/carbon dioxide+water systems changes the structure from SI to SII. Obviously, this is the reason why hydrate formation conditions change significantly. However, the effects of the addition of heavy hydrate formers into each system are not the same. The type of the help gas and also occupancy of heavy hydrate former into hydrate cavities dictates the final changes. The cage occupancy of benzene and cyclohexane requires further investigation using Raman spectroscopy or similar techniques.

CONCLUSIONS

The potential of heavy hydrate formers has been experimentally and theoretically presented in this study. An isochoric pressure search method was used to perform all the measurements. Experimental dissociation data for four phase hydrate equilibria (V-L$_{Aq}$-L$_{Hc}$-H) of methane+benzene+water, methane+cyclohexane+water, carbon dioxide+cyclohexane+water systems were measured and compared with literature data. Reliability of the experimental setup and the procedure of measurements was evaluated. Acceptable compatibility was observed between our data and literature data. Then, hydrate dissociation data of carbon dioxide+benzene+water four phase system were measured and presented.

Two well-known VPT+NDD and SAFT-HR EOSs were applied to predict the hydrate formation condition of the four phase equilibrium experimental data.

Kihara parameters of cyclohexane were obtained by adjusting to the hydrate dissociation data of methane/carbon dioxide/ethane+cyclohexane+water systems at ~275 K in this study.

Binary interaction parameters for each EOS were obtained from VLE and LLE data. Distortion of cages caused by the presence of large compounds is considered in modeling the hydrate phase. Considering distortion of cavities greatly improved the results. Comparison of the modeling results with experimental data shows that the results obtained by SAFT-HR EOS are in better agreement with the experimental data in comparison to VPT+NDD EOS at higher pressures.

ACKNOWLEDGEMENT

NOMENCLATURE

a : lattice parameter [Å]

C : Langmuir constant [kPa^{-1}]
f : fugacity [MPa]
H : hydrate
k : Boltzmann constant (1.38066×10^{-23} J K^{-1}), binary interaction parameter between nonpolar components in VPT+NDD and SAFT-HR EOSs
l : binary interaction parameter between polar and nonpolar component in VPT+NDD EOS
L$_{Aq}$: aqueous liquid
L$_{HC}$: hydrocarbon rich liquid
N : number of data
P : pressure [MPa]
r : distance of any point inside the cavity from the center of cavity [Å]
R : gas constant (8.314 MPa cm^3 K^{-1} mol^{-1})
Rs : radius of layer [Å]
T : temperature [K]
V : vapor
x : composition
X : any property
z : coordination number

Superscripts
cal : calculated value
exp : experimental value
hyd : hydrate phase
sat : saturated
vap : vapor phase
β : hypothetical empty hydrate phase
* : standard conditions at reference temperature, pressure and composition

Subscripts
i, j : component
m : cavity type
n : layer type
p : polar component
w : water
0 : standard conditions at reference temperature and pressure

Greek Letters
α : Kihara parameter- hard core radius [Å]
Δ : change in property
ε : Kihara parameter-depth of the intermolecular potential well [J^{-1}]
θ : fraction of occupied cavities by gas molecules
κ : compressibility constant [bar^{-1}]
K : pressure dependency of molar volume in an empty hydrate
λ : thermal expansivity constants [K^{-1}]
μ : chemical potential [J mol^{-1}]
v : number of certain type of cavities per water molecule, molar volume [cm^3 mol^{-1}]
σ : Kihara parameter- the soft core radius [Å]
φ : fugacity coefficient
ω : potential function between guest component and water molecules

REFERENCES

1. E. D. Sloan and C. Koh, *Clathrate Hydrates of Natural Gases*, Third Edition, CRC Press (2007).
2. K. K. Ostergaard, A. Danesh, A. C. Todd and R. W. Burgass, *Trans IChemE*, **78**, 731 (2000).
3. A. Danesh, B. Tohidi, R. W. Burgass and A. C. Todd, *Trans IChemE*, **71**, 457 (1993).
4. B. Tohidi, A. Danesh, R. W. Burgass and A. C. Todd, Effect of Heavy Hydrate Formers on the Hydrate Free Zone of Real Reservoir Fluids, in, Society of Petroleum Engineers (1996).
5. B. Tohidi, A. Danesh, A. R. Tabatabaei and A. C. Todd, *Ind. Eng. Chem. Res.*, **36**, 2871 (1997).
6. B. Tohidi, A. Danesh, A. C. Todd, R. W. Burgass and K. K. Østergaard, *Fluid Phase Equilib.*, **138**, 241 (1997).
7. K. A. Udachin, C. I. Ratcliffe and J. A. Ripmeester, *Hydrate structure and composition from single crystal X-ray diffraction: Examples of Str. I, II and H hydrates*, in: Fourth International Conference on Gas Hydrates, Domestic Organaizing Committee, ICGH-4, 2002, Yokohama, Japan, 604 (2002).
8. G. D. Holder, S. Zele and R. Enick, *Annals of the New York Academy of Sciences*, **715**, 344 (1994).
9. J. S. Tse, W. R. McKinnon and M. Marchi, *J. Phys. Chem.*, **91**, 4188 (1987).
10. S. R. Zele, S. Y. Lee and G. D. Holder, *J. Phys. Chem. B*, **103**, 10250 (1999).
11. R. A. Kini, Z. Huo, M. D. Jager, P. Bollavaram, A. L. Ballad, S. F. Dec and E. D. Sloan, Importance of Hydrate Phase Measurements in Flow Assurance and Energy, in: Fourth International Conference on Gas Hydrates, Domestic Organaizing Committee, ICGH-4, Yokohama, Japan, 867 (2002).
12. H. Tavasoli and F. Feyzi, *J. Natural Gas Sci. Eng.*, **24**, 473 (2015).
13. J. H. v. d. Waals and J. C. Platteeuw, Clathrate Solutions, in: Advances in Chemical Physics, John Wiley & Sons, Inc., 1 (1959).
14. A. L. Ballard and E. D. Sloan, Hydrate Separation Processes for Close-Boiling Compounds, in: Fourth International Conference on Gas Hydrates, Domestic Organaizing Committee, ICGH-4, Yokohama, Japan, 1007 (2002).
15. A. H. Mohammadi and D. Richon, *Chem. Eng. Sci.*, **66**, 4936 (2011).
16. P. J. Herslund, K. Thomsen, J. Abildskov, N. von Solms, A. Galfré, P. Brântuas, M. Kwaterski and J.-M. Herri, *International J. Greenhouse Gas Control*, **17**, 397 (2013).
17. J. A. Ripmeester, C. I. Ratcliffe and G. E. McLaurin, *The role of heavier hydrocarbons in hydrate formation*, in: AIChE. Spring Meeting, Session 44, Hydrates in the Gas Industry, Houston, TX (1991).
18. J. A. Ripmeester, S. T. John, C. I. Ratcliffe and B. M. Powell, *Nature*, **325**, 135 (1987).
19. A. H. Mohammadi, V. Belandria and D. Richon, *Ind. Eng. Chem. Res.*, **48**, 5916 (2009).
20. M. M. Mooijer-van den Heuvel, C. J. Peters and J. de Swaan Arons, *Fluid Phase Equilib.*, **172**, 73 (2000).
21. Z.-G. Sun, S.-S. Fan, K.-H. Guo, L. Shi, Y.-K. Guo and R.-Z. Wang, *J. Chem. Eng. Data*, **47**, 313 (2002).
22. B. Tohidi, A. Danesh, R. W. Burgass and A. C. Todd, *Chem. Eng. Sci.*, **51**, 159 (1996).
23. A. H. Mohammadi and D. Richon, *Chem. Eng. Sci.*, **64**, 5319 (2009).
24. M. M. Mooijer-van den Heuvel, R. Witteman and C. J. Peters, *Fluid Phase Equilib.*, **182**, 97 (2001).
25. M. Mohammad-Taheri, A. Zarringhalam Moghaddam, K. Nazari and N. Gholipour Zanjani, *Fluid Phase Equilib.*, **338**, 257 (2013).
26. R. Ohmura, S. Takeya, T. Uchida and T. Ebinuma, *Ind. Eng. Chem. Res.*, **43**, 4964 (2004).
27. B. Tohidi, R. W. Burgass, A. Danesh, K. K. ØStergaard and A. C. Todd, *Annals of the New York Academy of Sciences*, **912**, 924 (2000).
28. J. Valderrama, *J. Chem. Eng. Japan*, **23**, 87 (1990).
29. D. Avlonitis, A. Danesh and A. C. Todd, *Fluid Phase Equilib.*, **94**, 181 (1994).
30. S. H. Huang and M. Radosz, *Ind. Eng. Chem. Res.*, **29**, 2284 (1990).
31. S. H. Huang and M. Radosz, *Ind. Eng. Chem. Res.*, **30**, 1994 (1991).
32. S. Babaee, H. Hashemi, J. Javanmardi, A. Eslamimanesh and A. H. Mohammadi, *Fluid Phase Equilib.*, 336, 71 (2012).
33. A. Chapoy, I. Alsiyabi, J. Gholinezhad, R. Burgass and B. Tohidi, *Fluid Phase Equilib.*, **337**, 150 (2013).
34. D. Avlonitis, *Thermodynamics of gas hydrate equilibria*, in: Petroleum Engineering, Heriot-Watt University, Edinburgh, Scotland (1992).
35. A. Chapoy, Phase Behavior in Water/hydrocarbon Mixtures Involved in Gas Production Systems, in, Ecole Des Mines Paris Tech., Paris, France (2004).
36. M. W. Barrick, J. M. Anderson and R. L. Robinson, *J. Chem. Eng. Data*, **31**, 172 (1986).
37. J. J. Carroll, F.-Y. Jou, A. E. Mather and F. D. Otto, *Can. J. Chem. Eng.*, **76**, 945 (1998).
38. H. Chen and J. Wagner, *J. Chem. Eng. Data*, **39**, 470 (1994).
39. N. A. Darwish, K. A. M. Gasem and R. L. Robinson, Jr., *J. Chem. Eng. Data*, **39**, 781 (1994).
40. N. A. Darwish, K. A. M. Gasem and R. L. Robinson, *J. Chem. Eng. Data*, **43**, 238 (1998).
41. I. Gainar, The solubility of CO_2 and N_2O in some C_6 hydrocarbons at high pressures, Analele Universitatii Bucuresti: Chimie (2003).
42. A. Chapoy, A. H. Mohammadi, A. Chareton, B. Tohidi and D. Richon, *Ind. Eng. Chem. Res.*, **43**, 1794 (2004).
43. W. B. Kay and R. E. Albert, *Ind. Eng. Chem.*, **48**, 422 (1956).
44. C.-H. Kim, P. Vimalchand and M. D. Donohue, *Fluid Phase Equilib.*, **31**, 299 (1986).
45. Y. S. Kim, S. K. Ryu, S. O. Yang and C. S. Lee, *Ind. Eng. Chem. Res.*, **42**, 2409 (2003).
46. A. P. Kudchadker and J. J. McKetta, *AIChE J.*, **7**, 707 (1961).
47. E. N. Lay, V. Taghikhani and C. Ghotbi, *J. Chem. Eng. Data*, **51**, 2197 (2006).
48. D. Legret, D. Richon and H. Renon, *J. Chem. Eng. Data*, **27**, 165 (1982).
49. K. Lekvam and P. R. Bishnoi, *Fluid Phase Equilib.*, **131**, 297 (1997).
50. H.-M. Lin, H. M. Sebastian, J. J. Simnick and K.-C. Chao, *J. Chem. Eng. Data*, 24, 146 (1979).
51. A. Maczynski, D. G. Shaw, M. Goral, B. Wisniewska-Goclowska, A. Skrzecz, I. Owczarek, K. Blazej, M.-C. Haulait-Pirson, G. T. Hefter, Z. Maczynska, A. Szafranski and C. L. Young, *J. Phys. Chem. Reference Data*, **34**, 657 (2005).
52. T. Merker, N. Franke, R. Gläser, T. Schleid and H. Hasse, *J. Chem.*

Eng. Data, **56**, 2477 (2011).
53. D. J. Miller and S. B. Hawthorne, *J. Chem. Eng. Data*, **45**, 78 (2000).
54. A. H. Mohammadi, A. Chapoy, B. Tohidi and D. Richon, *Ind. Eng. Chem. Res.*, **45**, 4825 (2006).
55. B. J. Neely, J. Wagner, R. L. Robinson and K. A. M. Gasem, *J. Chem. Eng. Data*, **53**, 165 (2008).
56. M. P. W. M. Rijkers, M. Malais and C. J. Peters, J. de Swaan Arons, *Fluid Phase Equilib.*, **77**, 327 (1992).
57. E. P. Schoch, A. E. Hoffmann and F. D. Mayfield, *Ind. Eng. Chem.*, **32**, 1351 (1940).
58. P. Servio and P. Englezos, *Fluid Phase Equilib.*, **190**, 127 (2001).
59. K. Y. Song, G. Feneyrou, F. Fleyfel, R. Martin, J. Lievois and R. Kobayashi, *Fluid Phase Equilib.*, **128**, 249 (1997).
60. C. Tsonopoulos and G. M. Wilson, *AIChE J.*, **29**, 990 (1983).
61. A. Valtz, A. Chapoy, C. Coquelet, P. Paricaud and D. Richon, *Fluid Phase Equilib.*, **226**, 333 (2004).
62. L.-K. Wang, G.-J. Chen, G.-H. Han, X.-Q. Guo and T.-M. Guo, *Fluid Phase Equilib.*, **207**, 143 (2003).
63. Y. Wang, B. Han, H. Yan and R. Liu, *Thermochim. Acta*, **253**, 327 (1995).
64. J. B. Klauda and S. I. Sandler, *Ind. Eng. Chem. Res.*, **39**, 3377 (2000).
65. A. L. Ballard, *A non-ideal hydrate solid solution model for a multiphase equilibria program*, in, Colorado School of Mines (2002).
66. V. R. Belosludov, T. M. Inerbaev, O. S. Subbotin, R. V. Belosludov, J.-i. Kudoh and Y. Kawazoe, *J. Supramolecular Chem.*, **2**, 453 (2002).
67. B. C. Chakoumakos, C. J. Rawn, A. J. Rondinone, L. A. Stern, S. Circone, S. H. Kirby, Y. Ishii, C. Y. Jones and B. H. Toby, *Canadian J. Phys.*, **81**, 183 (2003).
68. T. Ikeda, S. Mae, O. Yamamuro, T. Matsuo, S. Ikeda and R. M. Ibberson, *J. Phys. Chem. A*, **104**, 10623 (2000).
69. S. Takeya, H. Fujihisa, A. Hachikubo, H. Sakagami and Y. Gotoh, *Chem. - A European J.*, **20**, 17207 (2014).
70. T. A. Strobel, C. A. Koh and E. D. Sloan, *Fluid Phase Equilib.*, **280**, 61 (2009).
71. E. D. Sloan, K. A. Sparks and J. J. Johnson, *Ind. Eng. Chem. Res.*, **26**, 1173 (1987).
72. S. Saito, D. R. Marshall and R. Kobayashi, *AIChE J.*, **10**, 734 (1964).
73. W. R. Parrish and J. M. Prausnitz, *Ind. Eng. Chem. Process Design Development*, **11**, 26 (1972).
74. G. D. Holder and J. H. Hand, *AIChE J.*, **28**, 440 (1982).
75. L. Lundgaard and J. Mollerup, *Fluid Phase Equilib.*, **76**, 141 (1992).
76. D. Avlonitis, *Chem. Eng. Sci.*, **49**, 1161 (1994).
77. A. P. Mehta and E. D. Sloan, *AIChE J.*, **42**, 2036 (1996).
78. E. D. Sloan, Clathrate Hydrates of Natural Gases, Second Edition, Revised and Expanded, Taylor & Francis (1998).
79. M. M. Mooijer-van den Heuvel, phase behavior and structural aspects of ternary clathrate hydrate systems. The role of additives, in, Technical universiteit Delf (2004).
80. I. B. A. Sfaxi, V. Belandria, A. H. Mohammadi, R. Lugo and D. Richon, *Chem. Eng. Sci.*, **84**, 602 (2012).
81. F. E. Anderson and J. M. Prausnitz, *AIChE J.*, **32**, 1321 (1986).
82. M. Illbeigi, A. Fazlali and A. H. Mohammadi, *Ind. Eng. Chem. Res.*, **50**, 9437 (2011).
83. J. A. Ripmeester and C. I. Ratcliffe, *J. Phys. Chem.*, **94**, 8773 (1990).
84. T. Nakamura, T. Makino, T. Sugahara and K. Ohgaki, *Chem. Eng. Sci.*, **58**, 269 (2003).
85. T. Maekawa, *Fluid Phase Equilib.*, **267**, 1 (2008).
86. K. Tumba, P. Reddy, P. Naidoo, D. Ramjugernath, A. Eslamimanesh, A. H. Mohammadi and D. Richon, *J. Chem. Eng. Data*, **56**, 3620 (2011).